Control of an Optimal Finger Exoskeleton based on Continuous Joint Angle Estimation from EMG signals

Jimson Ngeo[1], Tomoya Tamei[1], Tomohiro Shibata[1],
M.F. Felix Orlando[2], Laxmidhar Behera[2], Anupam Saxena[3], and Ashish Dutta[3]

Abstract—**Patients suffering from loss of hand functions caused by stroke and other spinal cord injuries have driven a surge in the development of wearable assistive devices in recent years. In this paper, we present a system made up of a low-profile, optimally designed finger exoskeleton continuously controlled by a user's surface electromyographic (sEMG) signals. The mechanical design is based on an optimal four-bar linkage that can model the finger's irregular trajectory due to the finger's varying lengths and changing instantaneous center. The desired joint angle positions are given by the predictive output of an artificial neural network with an EMG-to-Muscle Activation model that parameterizes electromechanical delay (EMD). After confirming good prediction accuracy of multiple finger joint angles we evaluated an index finger exoskeleton by obtaining a subject's EMG signals from the left forearm and using the signal to actuate a finger on the right hand with the exoskeleton. Our results show that our sEMG-based control strategy worked well in controlling the exoskeleton, obtaining the intended positions of the device, and that the subject felt the appropriate motion support from the device.**

I. INTRODUCTION

Given the dominant role of the human hand, where many everyday functional tasks are achieved by our hands, hand finger injuries can be a serious problem. Spinal cord injuries and stroke, which can lead to partial paralysis of the hand while the brain is still active can impede important daily human functions. Rehabilitation is often the solution to help restore proper functions even if it is costly, time-consuming, and needs sufficient access to therapists and equipments available only in special places. One practical alternative is to provide robotic assistance in the form of hand exoskeletons that can give tireless support [1]. Additionally, for current hand exoskeletons to allow maximum function, it must also be able to replicate fine and continuous hand finger motions.

Many hand exoskeletons systems have been proposed and constructed, both in the past and recently. These can generally be described and differentiated by their mechanical design, number of degrees of freedom possible, choice of actuators, or the chosen control strategies. Of the exoskeleton designs, some have revolute joints which are simple in design but do not follow precise human finger trajectory. While others provide multiple finger support with a large number of degrees-of-freedom (DOF) but are mechanically complex, bulky and requires high power to drive all the actuators simultaneously. Some designs have also used pulley and cable-driven transmission mechanisms to reduce contactable parts in the hands that may impede natural hand movements and to provide comfort and low-weight to the users. However, the drive systems of such cable systems at the back-end tend to be very large and heavy.

Control strategies based on surface electromyographic (sEMG) signals have often been used in robotic interfaces and hand prosthetic control because these reflect the motor intention of users very well [2]. There has been great success in discrete classification of hand gestures reaching accuracies of above 90% [3]. There have also been many reports on the use of sEMG in gait, upper limb and wrist rehabilitation. However, applications specifically related to continuous hand and finger movements based on sEMG have been very few.

Choi et al. have designed a finger exoskeleton based on a four-bar link that allows maximum freedom of each finger [4]. Their exoskeleton provided directional forces in the dorsal and palmar direction of the hand but have not compared their design's movement to actual human finger trajectories. Sands et al. have also designed a reconfigurable mechanism for finger rehabilitation based on the four-bar design [5]. More recently, Orlando et. al. have created an optimal four-bar linkage design of the index finger based on recorded human finger trajectories [6]. They have used sEMG signals to discriminate hand positions, in a 1-second window time frame which is quite slow, to control their exoskeleton. The four-bar linkage design has however been carefully selected because of its ability to model recorded human finger point trajectories. This is particularly difficult to do with a human finger joint, because it does not follow a simple revolute joint with a fixed pivot center point, but whose instantaneous center changes during finger motion.

In this paper, we present an optimal design and sEMG-based control of a portable 3 DOF per finger exoskeleton that can allow fine continuous finger movements. Hand exoskeletons are normally grounded on the user's body and must be as light as possible. Also, the device must be able to reflect appropriate forces on the hand, which was not achieved in Orlando's previous work. Both the mechanical design and control approach of our system is designed to be

[1] J. Ngeo, T. Tamei, and T. Shibata are with the Graduate School of Information Science, Nara Institute of Science and Technology, 8916-5 Takayama, Ikoma City, Nara 630-0192, Japan. {jimson-n, tomo-tam, tom}@is.naist.jp

[2] M.F. Orlando and L. Behera are with the Department of Electrical Engineering, Indian Institute of Technology Kanpur, 208016, India. {mfelixor, lbehera}@iitk.ac.in

[3] A. Saxena and A. Dutta are with the Department of Mechanical Engineering, Indian Institute of Technology Kanpur, 208016, India. {anupams, adutta}@iitk.ac.in

easily scalable to fit different users, use relatively low-power, and compact in size which is intended for both clinical or home use. To allow easy customization for new subjects, a modified design of the optimal four-bar linkage exoskeleton based on Orlando's previous work was developed. Our sEMG control strategy makes use of an EMG-to-Muscle Activation model as input to an artificial neural network that can predict multiple finger joint angles simultaneously. Using the said model is best suited for such a regression problem, because it requires only a few parameters, but most importantly considers electromechanical delay (EMD), which is inherent in sEMG-related motion applications.

II. METHOD

### A. Construction of the Finger Exoskeleton Based on an Optimal Four-bar Linkage Design

The construction of the exoskeleton can be summarized into the following steps. First, a motion capture system was used to collect finger flexion and extension joint trajectories. Second, using selected points from the complete finger joint trajectory, a 3-point motion generation by analytical synthesis was used to generate an initial four-bar linkage design. Kinematic and constraint equations for the four-bar mechanism were defined in this step. Third, an optimization procedure was done in order to find the design parameters (e.g. the link lengths and pivot positions) that would minimize the mean-squared error between the recorded finger trajectory and the generated four-bar trajectory. Lastly, once the optimal lengths and positions of linkage have been determined, a 3D CAD model is created to which prototyping of the components with a 3D printer follows next.

In collecting the finger joint trajectory, three reflective markers positioned in the form of a coupler triangle in each finger phalanx, and one marker for each of the remaining joints were attached on the index and thumb finger of a subject (see figure 1a). The subject was tasked to perform flexion and extension motion of the three finger joints, the metacarpophalangeal (MCP), proximal interphalangael (PIP) and the distal interphalangeal (DIP) joints. While finger movements were made, the marker positions were recorded using a MAC3D motion capture system (Motion Analysis Corp.) with sampling frequency of 200 Hz and measurement units in millimeter, having a precision of 0.5 mm. Finger flexion and extension movements are best described as when any finger curls up to form a fist or uncurls to form the opening of the palm, respectively. The design of the exoskeleton was made in such a way that the linkages allow 3 DOF per finger, one for each finger joint, to move in the flexion and extension plane.

Each phalanx of a finger is modeled as a four-bar linkage as shown in figure 1 with P representing the finger joint trajectory. The parameters that we want to obtain in this design problem are the pivot positions O_2 and O_4 and the four-bar link lengths W, V, U, G, with the corresponding position angles θ, ϕ, σ, and ψ. An initial four-bar design is computed based on the 3 point trajectories given by P_1, P_2, P_3 and their corresponding positions angles, and

(a) Reflective markers on two fingers
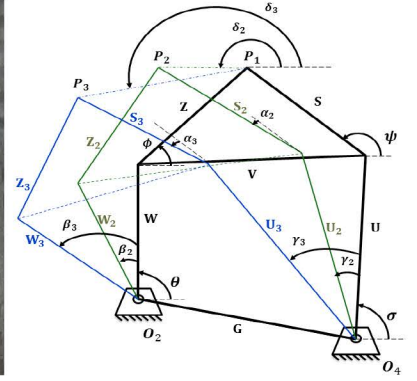
(b) Four-bar Linkage

Fig. 1: Motion marker placement and the general four-bar linkage mechanism.

whose kinematic equations can be derived if the links are represented in vector loop equations taken from both the left and right side of the linkage [7]:

$$\mathbf{W_2} + \mathbf{Z_2} - \mathbf{Z} - \mathbf{W} = \mathbf{P_{21}} \tag{1}$$

$$\mathbf{W_3} + \mathbf{Z_3} - \mathbf{Z} - \mathbf{W} = \mathbf{P_{31}} \tag{2}$$

$$\mathbf{U_2} + \mathbf{S_2} - \mathbf{S} - \mathbf{U} = \mathbf{P_{21}} \tag{3}$$

$$\mathbf{U_3} + \mathbf{S_3} - \mathbf{S} - \mathbf{U} = \mathbf{P_{31}} \tag{4}$$

Using *Euler's Identity*, a system of equations can be derived from which the link lengths W, Z, S, and U can be computed. The equation for output angle σ and the coupler angle ψ can also be derived,

$$\sigma = 2\arctan\left[\frac{(A-\sqrt{A^2+B^2-C^2})}{B+C}\right] \tag{5}$$

$$\psi = 2\arctan\left[\frac{(A+\sqrt{A^2+B^2-D^2})}{B+D}\right] \tag{6}$$

where A, B, C and D are given by,

$$A = \sin\theta - \frac{G}{U}\sin\delta \tag{7}$$

$$B = \cos\theta - \frac{G}{U}\cos\delta \tag{8}$$

$$C = \frac{G}{W}\cos(\theta - \delta) + \frac{(G^2+U^2+W^2-V^2)}{2WV} \tag{9}$$

$$D = -\frac{G}{V}\cos(\theta - \delta) + \frac{(G^2+U^2+V^2-W^2)}{2UV} \tag{10}$$

Constraints were also placed to ensure that the four-bar link lengths and the pivot points are confined within an allowable region, which is a small rectangular area on top of each joint. This ensures that the design is compact and that the exoskeleton occupies only the dorsal region of the hand.

An optimization procedure was then carried out to determine the optimal length of four-bar links for a specific user by minimizing a square error function between the recorded human finger trajectory and the joint trajectory generated by the linkage model. Once the optimal lengths and position of the linkages were determined and checked if the overall dimension of the exoskeleton would fit in the hand, a 3D CAD model was then created in Autodesk Inventor and rapid prototypes were built using a 3D printer.
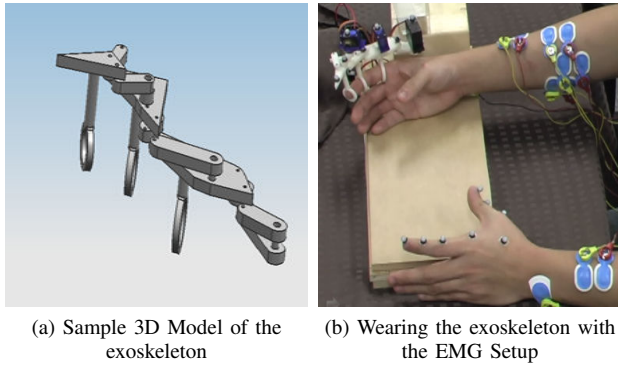
(a) Sample 3D Model of the exoskeleton

(b) Wearing the exoskeleton with the EMG Setup

Fig. 2: Constructed Index Finger Exoskeleton.

Fig. 3: Organization of the building and control of the finger exoskeleton system.

This customized finger exoskeleton is designed to be portable and low-powered, which must be suitable for both clinical or personal use. To actuate and control the finger exoskeleton, an inexpensive Arduino Mega micro-controller was used to send the processed EMG motor commands to the exoskeleton. To actuate the MCP, PIP and DIP joints using the current prototype, a GWS Micro-MG and two MiniS RB90 mini RC servo with rated torques of 5.4 kg-cm and 1.6 kg-cm, respectively, was used due to its high power-to-weight ratio. To help support the exoskeleton, which weighed about 50 grams, an external support was added.

B. Continuous Joint Angle Estimation from EMG

To control the exoskeleton, surface EMG signals from the user were used to predict the motor intention of continuous moving fingers. Four extrinsic muscles in the forearm that are known to contribute to finger movements were selected. These muscles are the Flexor Digitorum Superficialis (FDS), Flexor Digitorum Profundus (FDP), Extensor Digitorium (ED), and the Extensor Indices (EI). The sEMG signals were recorded using a compact BA1104 electromyograph with active-type (Ag/AgCl) electrodes and interelectrode distance of 20 mm, and a telemetry unit TU-4 (Digitex Laboratory Co. Ltd.). The hardware provided a high-pass filter with cut-off frequency of 1 kHz during the data acquisition process. To match the frequency of the motion data, the EMG signals were also sampled at 200 Hz. For any intended motor action, it is known that there occurs a time delay, which is known as the electromechanical delay (EMD), between the onset of the sEMG signals and the exerting tension in the muscles. EMD has been observed by previous studies in the leg and as well as in the arm [8][9]. To learn a suitable filtered signal which automatically considers EMD, we introduce the use of a so called EMG-to-Muscle Activation model. SEMG is a measure of electrical activity that spreads across muscles, which causes the muscles to activate. This results to the production of force, to which the model used transforms the sEMG signals to a suitable force representation. Buchanan et al. created a second-order model filter that works efficiently to model the relationship between EMG and muscle activation [9]. In this study, we make use of their filter given by:

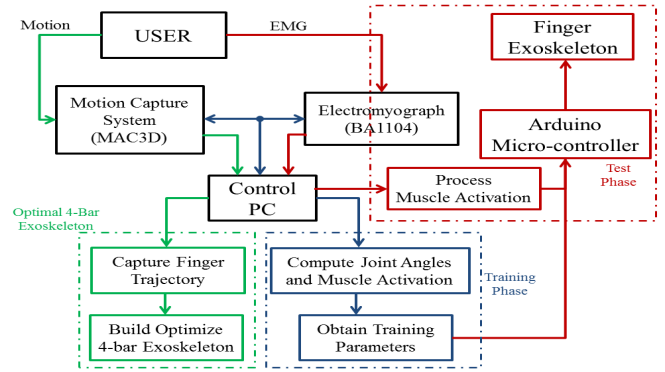$$u_j(t) = Le_j(t-d) - B_1 u_j(t-1) - B_2 u_j(t-2) \qquad (11)$$

where $e_j(t)$ is the rectified, low-pass filtered, and normalized EMG of muscle j at time t, In this model, L, B_1, B_2 are recursive coefficients and d is the EMD. Filter stability is guaranteed by putting constraint conditions:

$$B_1 = C_1 + C_2 \qquad (12)$$
$$B_2 = C_1 \cdot C_2 \qquad (13)$$
$$|C_1| < 1, |C_2| < 1 \qquad (14)$$
$$L - B_1 - B_2 = 1 \qquad (15)$$

The transformation to muscle activation v_j is given by:

$$v_j = \frac{e^{A_j u_j(t)} - 1}{e^{A_j} - 1} \qquad (16)$$

where A_j is a parameter that introduces the nonlinearity between EMG and muscle activation, and is constrained between -3 (highly exponential) and 0 (linear).

Because there is no clear relationship between the muscle activation and the produced finger joint angles, we use an artificial neural network as the estimator because of its ability to approximate any nonlinear arbitrary functions [10]. In this study, a feed-forward neural network made up of 3 layers: an input layer with 4 nodes coming from the target muscles, a single hidden layer with a tan-sigmoidal activation function, and a single linear output layer with 3 to 6 nodes, which are the joint angles that we want to predict, was used. The network's performance was evaluated with various number of neurons in the hidden layer, ranging from 5 to 250.

The use of the muscle activation model not only considers the EMD present in such sEMG-based motion applications, but also requires only a few parameters. The parameters of the filter, C_1, C_2, d, A and along with the weight parameters of the neural network were obtained through optimization by minimizing a mean square error function given by:

$$\sum_t \frac{1}{n} (Y_{est} - Y_{target})^2 \qquad (17)$$

where Y_{est} and Y_{target} are the estimated and measured finger joint angles, respectively and n is the number of samples used to train the network. Various number of neurons in the hidden layer were evaluated and an early stopping method was applied during training iterations.
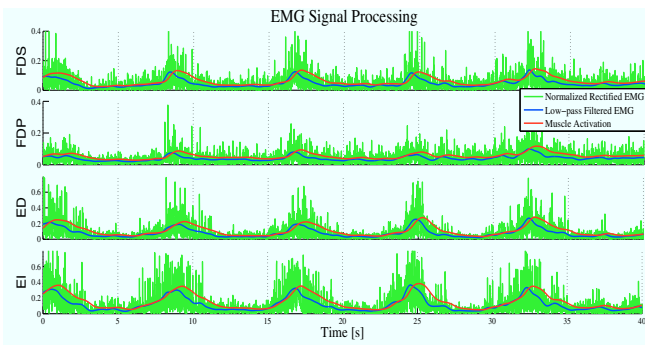
Fig. 4: Obtaining the muscle activation inputs from EMG.

Fig. 5: EMG and index finger joint angle estimation result.

III. EXPERIMENTS: SYSTEM EVALUATION

After obtaining the neural network and muscle activation parameters, we estimated the index finger MCP, PIP and DIP joint angles simultaneously. To evaluate the system, a healthy male subject (age 26 and right-handed) wore a customized finger exoskeleton on his right hand (see figure 2b), while EMG signals were obtained from his left hand. The subject was asked to flex and extend his left index finger, with the rest of the hand in neutral position, while the right index finger was actuated by the exoskeleton following the movements of the left. The subject maintained no movement in the right finger to let the exoskeleton assist in the movement.

A joint angle test prediction result is shown (see figure 5), when the EMG was transformed into its muscle activation (see figure 4) and used as input to predict the index finger joint angle. The blue plot shows the measured joint angle obtained from the left index finger, while the red plot shows the predicted joint angle from the regressor. The green plot shows the actuated motion of finger exoskeleton on the right index finger. Correlation as high as 0.9 and root-mean-square percentage error of less than 10% were obtained between the predicted and estimated index finger MCP joint angles. Prediction of the PIP and DIP joint angles also gave reasonable results with correlations of above 0.75 and 0.7, respectively. However in some trials, the PIP and DIP angles were not as accurate as in predicting the MCP joint angles. One likely reason for this is that only extrinsic muscles were targeted. A huge variety of finger movements involving the PIP and DIP angles are actuated by deep intrinsic muscles which are harder to access.

The predicted finger joint angles were enough to actuate the exoskeleton and to continuously assist finger flexion and extension movement. The subject felt that enough support was given to his right index finger and that the actuation of the exoskeleton was almost about the same time as the movement execution of the left index finger.

IV. CONCLUSION

This study presented an alternative and improved method in controlling an optimal four-bar linkage based finger exoskeleton using surface EMG signals. Using an EMG-to-muscle activation model as input to a regressor gave good estimation accuracy in predicting multiple finger joint angles
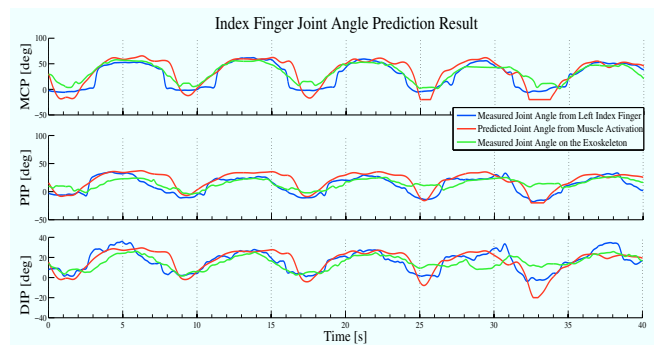
simultaneously and was tested in a real-time application setting. Our proposed sEMG-based control strategy was effective on the exoskeleton when used as a prosthesis, accurately obtaining the intended positions of the device. This is but only a step closer to reaching our ultimate goal of providing hand and finger rehabilitation with our designed exoskeleton. In the future, we plan to extend the design to add more fingers, increase the number of target subjects and explore other control strategies. Strategies such as an "assist-as-needed" type of control may be more suitable for rehabilitation, which can potentially allow maximum functional recovery through the use of robotic assistive devices.

V. ACKNOWLEDGMENTS

REFERENCES

[1] B. Dellon and Y. Matsuoka, "Prosthetics, exoskeletons, and rehabilitation," in *IEEE Robotics and Automation Magazine*, 2007.

[2] L. Lucas, M. DiCicco, and Y. Matsuoka, "An emg-controlled hand exoskeleton for natural pinching," *Journal of Robotics and Mechatronics*, vol. 16, pp. 482–488, 2004.

[3] M. Zecca, S. Micera, M. Carrozza, and P. Dario, "Control of multifunctional prosthetic hands by processing the electromyographic signal," *Crit. Reviews in Biomedical Engineering*, vol. 30, pp. 459–485, 2002.

[4] B. Choi and H. Choi, "A semi-direct drive hand exoskeletons using ultrasonic motor," in *Proceedings of the 1999 IEEE International Workshop on Robot and Human Interaction*, pp. 285–299, IEEE, 1999.

[5] D. Sands, A. Perez, J. McCormack, and E. Wolbrecht, "Design method for a reconfigurable mechanism for finger rehabilitation," in *15th IASTED Int. Conf. on Robotics and Applications*, pp. 1–8, 2010.

[6] M. Orlando, H. Akolkar, A. Dutta, A. Saxena, and L. Behera, "Optimal design and control of a hand exoskeleton," in *2010 IEEE Conference on Robotics, Automation and Mechatronics (RAM)*, IEEE, 2010.

[7] R. Norton, *Design of machinery: an introduction to the synthesis and analysis of mechanisms and machines*. McGraw-Hill, 2004.

[8] N. Shrirao, N. Reddy, and D. Kosuri, "Neural network committees for finger joint angle estimation from surface emg signals," *Biomedical Engineering Online*, vol. 8(2), pp. 1–11, 2009.

[9] T. Buchanan, D. Lloyd, K. Manal, and T. Besier, "Neuromusculoskeletal modeling: Estimation of muscle forces & joint moments and movements from measurements of neural command," *Journal of Applied Biomechanics*, vol. 20(4), pp. 367–395, November 2004.

[10] B. Csaji, "Approximation with artificial neural networks," 2001.